

Spanwise Response Variation for Partial-Span Gurney-Type Flaps

Stephen A. Solovitz* and John K. Eaton†
Stanford University, Stanford, California 94305

Uninhabited air vehicles with high-aspect-ratio wings can experience substantial aeroelastic modes, which can adversely affect performance. An active, distributed control system is being developed to alleviate these vibrations, using a series of small span trailing-edge actuators to alter the aerodynamic loads at specific spanwise locations. Particle image velocimetry was used to determine the spanwise effects of these devices because it is necessary to understand whether their application will have nonlocal effects. The wake structure indicates that the primary influence is confined to within two actuator spans of the applied device, demonstrating that the response is quite localized.

Nomenclature

b	= wing span, 87.9 cm
C_L	= coefficient of lift normalized by wing planform area, $L/(1/2\rho U_\infty^2 bc)$
C_l	= section coefficient of lift
c	= airfoil chord length, 60.2 cm
L	= lift
Re_c	= Reynolds number based on chord length, $U_\infty c/\nu$
U_∞	= flow velocity
u'	= instantaneous streamwise fluctuation velocity
w'	= instantaneous wing-normal fluctuation velocity
x	= streamwise position (origin at the airfoil leading edge)
y	= spanwise position (origin at the center of a midspan device)
z	= wing-normal position (origin at the chordline)
α_{app}	= approximate downwash scalar
ν	= kinematic viscosity
ρ	= fluid density

Subscripts

max	= maximum value of quantity
press	= pressure side of airfoil
suct	= suction side of airfoil
TE	= trailing edge

Superscript

—	= ensemble averaged
---	---------------------

I. Introduction

HIGH-ALTITUDE endurance uninhabited air vehicles (UAVs) require high-aspect ratio, low-stiffness wings to meet performance specifications. Because of these properties, the aircraft are susceptible to significant aeroelastic vibrations, which can result in a loss of control. Whereas traditional control techniques are effective for low-frequency and low-order modes, they are not suitable for these UAVs, which experience higher-order vibrations. A new aerodynamic control approach is necessary to satisfy the requirements of high temporal and spatial bandwidth.

Received 13 February 2003; revision received 27 January 2004; accepted for publication 2 February 2004. Copyright © 2004 by the American Institute of Aeronautics and Astronautics, Inc. All rights reserved. Copies of this paper may be made for personal or internal use, on condition that the copier pay the \$10.00 per-copy fee to the Copyright Clearance Center, Inc., 222 Rosewood Drive, Danvers, MA 01923; include the code 0001-1452/04 \$10.00 in correspondence with the CCC.

*Graduate Research Assistant, Department of Mechanical Engineering; currently Mechanical Engineer, General Electric Global Research, One Research Circle, Niskayuna, NY 12309.

†Professor, Department of Mechanical Engineering, Building 500, Room 501F, 488 Escondido Mall. Senior Member AIAA.

A multidisciplinary group at Stanford University^{1,2} is investigating a distributed flow control technique that can meet these requirements. The idea is based on the Gurney flap, a small trailing-edge flap on the order of 1% of the airfoil chord mounted at 90 deg to the chord. Because of the large deflection angle, there is a significant increase in the lift and nose-down pitching moment. However, the drag penalties are relatively small due to the small scale of the device. When the Gurney flap is divided into many smaller segments [micro-trailing-edge effectors (MiTEs)], each individually controlled, it is possible to alter locally the aerodynamic loads. When an appropriate actuation pattern is chosen, the aeroelastic vibrations could be suppressed, as was demonstrated analytically by Lee et al.¹ Because of the small size and great number of these MiTEs, this control design would have advantages of simplicity, high bandwidth, great pattern variety, and redundancy.

Previous experiments² showed that MiTEs could produce a significant lift increment (± 0.25 for full-span actuation), whose magnitude varied linearly with the length of the actuated span, which suggested that the response could be modeled easily. In addition, the load increments superposed linearly regardless of whether there were gaps between the devices. However, streamwise pressure profiles indicated that there was a significant nonlocal effect when a single MiTE was applied. The greatest effect on the section lift coefficient was localized within about 3 device spans, but there was still a noticeable influence on the pressure profiles as much as 10 flap spans away. The magnitude of this distant effect was smaller than the uncertainty in C_l due to the uncertainty in wing angle of attack, and so it was impossible to be conclusive about the true extent of the spanwise influence. To develop an effective control system, the spanwise influence must be determined because the devices are intended to promote localized changes in the aerodynamics. Therefore, other measurement techniques were necessary to determine the spanwise variation in the aerodynamic effects.

One effective method of examining the spanwise response is measurement of the wake flow structure through particle image velocimetry (PIV). The basic wake structure for a Gurney flap was first postulated by Liebeck.³ He suggested that the mean flow consisted of a recirculating region upstream of the flap and a pair of counter-rotating vortices downstream of the device. When the Gurney flap was applied, the flow remained attached on the suction surface at higher lift conditions, allowing an increase in C_L . Jang et al.⁴ verified this hypothesis using INS2D computations. Jeffrey et al.⁵ used laser Doppler anemometry (LDA) to examine quantitatively the flow structure behind a Gurney flap, again matching Liebeck's postulate. However, they noted that this was only the time-averaged structure, not the instantaneous case. The actual structure consisted of bluff-body shedding behind the flap, which was visualized with smoke. Zerihan and Zhang⁶ showed this shedding more quantitatively using PIV measurements, which was the first use of this technique to study Gurney flaps. Still, there has been no examination of the flow structure for partial-span Gurney flap devices, such as MiTEs. The specific objective of this work is to determine

the region of influence of a partial-span Gurney flap by examining the wake structure at various spanwise positions.

II. Experimental Apparatus

The experiments were conducted in the Stanford Flow Control Wind Tunnel, which is a subsonic (0–22-m/s) closed-loop wind tunnel with excellent flow uniformity and freestream turbulence below 0.5%. The test section is 61 cm wide \times 91 cm high \times 4 m long. A two-dimensional airfoil model with a MESO5 profile was mounted vertically in the test section (Fig. 1a), spanning the tunnel height. The design chord length for the airfoil was 61.0 cm, but 3.3 cm was trimmed from its trailing edge to provide a blunt base (6.5 mm thick) for MiTE attachment. The flap mounting manifold extended 2.5 cm from this blunted surface, so that the actual airfoil chord length was $c = 60.2$ cm. A boundary-layer trip was installed at a position 12.6% of the chord length downstream of the leading edge on both the pressure and suction surfaces to provide uniform transition to turbulence.

There were 16 MiTEs attached to the blunt trailing edge around the spanwise midpoint. These devices had a 31-mm span, and when

actuated, they extended from the wing surface by 9 mm, corresponding to 1.5% of the wing chord. These flaps were designed by Park in the Stanford Rapid Prototyping Laboratory, and the details of their development and manufacturing are described in Ref. 7. Each MiTE was operated independently by a small dc motor, which actuated a rack-and-pinion linkage that moved the flap. The devices could be operated at frequencies in excess of 17 Hz. In their present configuration, these flaps could move between two positions, fully up or fully down (at 90 deg to the suction or pressure surface, respectively). A third, neutral position, where the flap was mostly hidden behind the blunt trailing edge, was also used. In this position, the flap protruded 1.25 mm beyond both the suction and pressure surfaces of the wing. The 16 functional flaps only occupied the central 48 cm of the wing span. Stationary flaps with the same 9-mm chord length were mounted over the remainder of the span to simulate MiTEs uniformly actuated in one direction.

The flow structure in the near wake was analyzed through PIV interrogation with a standard commercial TSI system, as shown in Fig. 1b. The test region was illuminated with a Spectra-Physics Nd:YAG PIV 400 dual-head laser located outside the tunnel. The beam passed through an articulated arm to the laser sheet optics, which produced a laser sheet centered on a midspan MiTE. The sheet passed just downstream of the trailing edge, allowing examination of a window extending about 7% of the chord past the wing and $\pm 2.5\%$ of the chord on either side. The flow was seeded using a Rosco Delta 3000 fog generator placed at the downstream end of the test section, approximately 3 m past the wing. The generator produced a fine mist of particles by vaporizing a glycerol, which recondensed into droplets on the order of $0.3 \mu\text{m}$ in diameter. These particles circulated back through the tunnel blower, providing a uniform dispersion of droplets in the interrogation region. The region was imaged using a TSI PIVCAM 13-8 charge-coupled device camera located beneath the tunnel. The entire PIV system was controlled using a synchronizer operated with Insight software. The images were analyzed using Pivlab2000, an iterative processing program developed by Han.⁸ For this configuration, the smallest interrogation region was 0.6 by 0.6 mm, and the uncertainty in measured velocity was $\pm 0.9\%$. The uncertainty in the Reynolds normal stresses was $\pm 13\%$.

III. Results

The first experiments considered full-span cases because these were the only cases where the flow structure had been studied quantitatively in previous experiments. The wing was oriented at an angle of attack of 0.57 deg, and the Reynolds number was fixed at $Re_c = 9.0 \times 10^5$. For each condition, 1000 image pairs of PIV data were acquired.

First, all of the MiTEs were fixed in the neutral position. Figure 2a shows the mean velocity vectors for this condition, obtained by ensemble averaging all 1000 measured velocity fields. The structure consists of a separation bubble extending from the blunt trailing edge to approximately $x/c = 1.03$, bounded on either side by shear layers. In the mean, the separated flow contains two counter-rotating vortices of similar size and strength. This basic structure is very similar to that expected for blunt trailing edges.⁹

Note that, in the neutral position, there was some slight overhang from the actual blunted surface, with the shear layers emanating from the ends of the flap. This overhang does lead to a drag penalty. However, this generation of MiTEs was simply designed to demonstrate and study their basic effects. It is possible to develop devices that do not have these features, and future MiTE generations will be designed in that manner.

The time-averaged wake flow for the fully down position is shown in Fig. 2b. In this case, all of the MiTEs and fixed flaps were actuated downward toward the pressure surface. The flow still shows a pair of vortices, but the locations and shapes are different. The suction-side vortex increased in size, extending farther downstream and more toward the pressure surface. The pressure-side vortex shifted off of the surface of the wing, and it decreased in size. The separated region extended farther downstream, and the off-surface stagnation point shifted toward the pressure side, indicating higher downwash and,

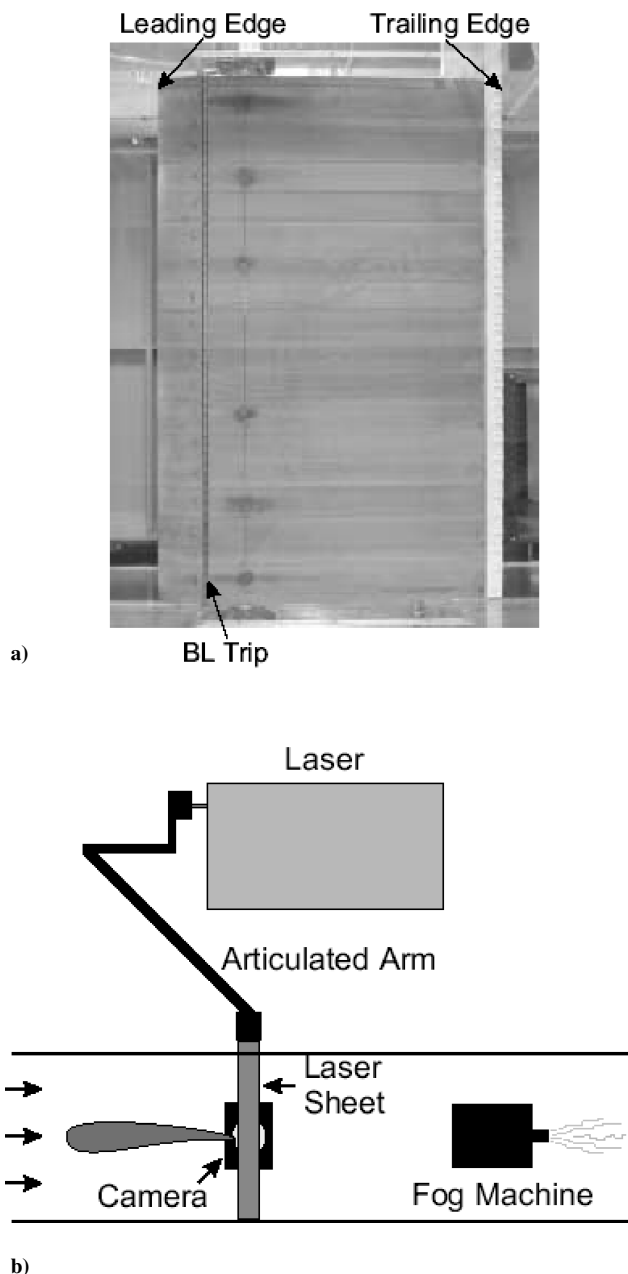
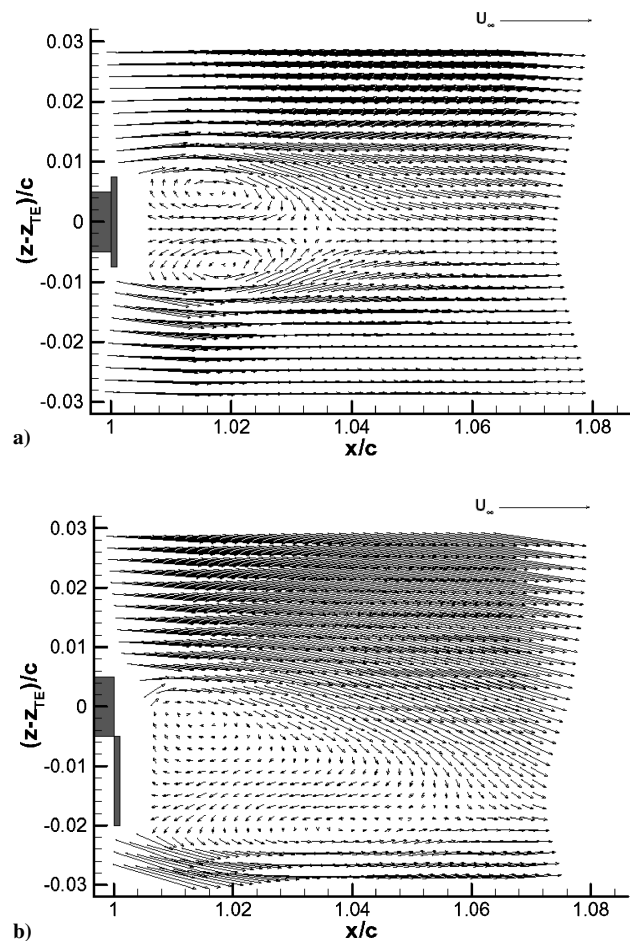


Fig. 1 Experimental apparatus: a) wing installed in wind tunnel (side view) and b) schematic of PIV system (top view).

Table 1 Quantitative flow statistics from PIV measurements for full- and partial-span conditions

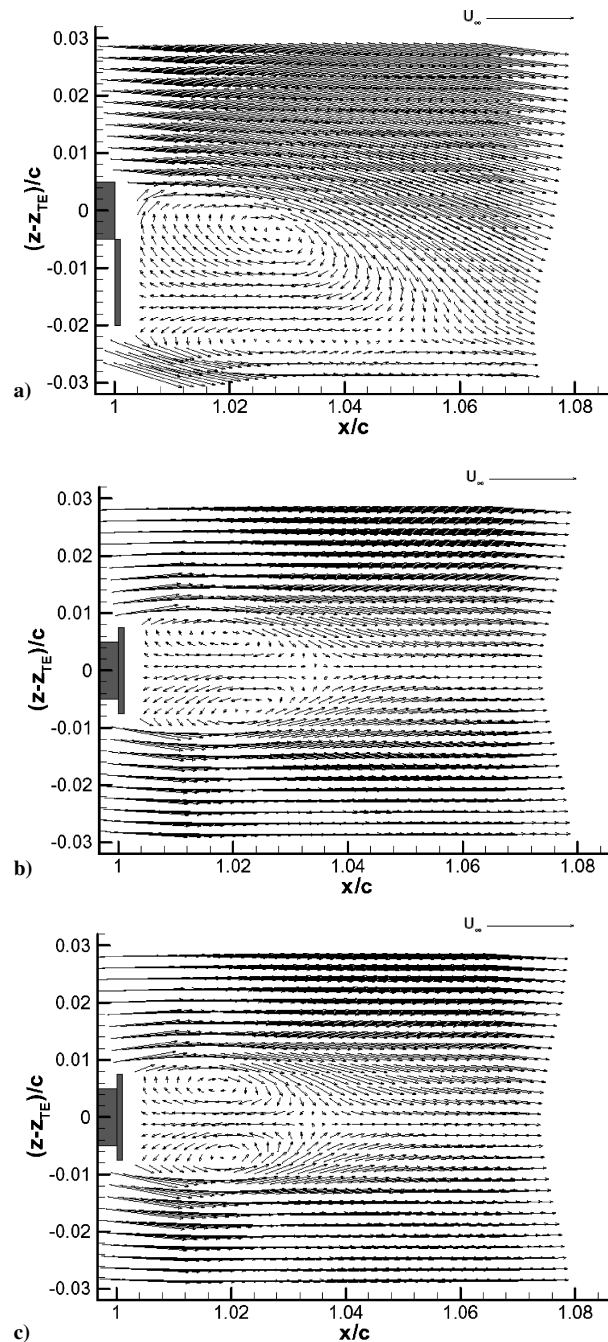
Condition	α_{app} , deg	$\overline{u_{suct,max}^2} / U_\infty^2$	$\overline{u_{press,max}^2} / U_\infty^2$	$\overline{w_{max}^2} / U_\infty^2$
Neutral	-2.4	0.059	0.094	0.054
Down	-12.1	0.041	0.132	0.081
$ y - y_{flap} /b = 0$	-15.9	0.049	0.137	0.059
$ y - y_{flap} /b = 0.037$	-1.3	0.056	0.101	0.042
$ y - y_{flap} /b = 0.073$	-1.6	0.049	0.068	0.051

**Fig. 2** Full-span wake structure: a) neutral position, mean velocity flowfield, and b) down position, mean velocity flowfield.

thus, lift. This time-averaged flow was comparable to the postulated flow of Liebeck,³ the computations of Jang et al.,⁴ and the LDA experiments of Jeffrey et al.⁵

Figures 2a and 2b show the time-averaged wake structure, but in actuality the individual instantaneous vector plots did not show the same clear vortical structures in this unsteady flow. In each instantaneous field, there were large vortices similar to the bluff-body shedding seen by Jeffrey et al.⁵ alternating in sign and offset in location. The individual PIV fields were not phase locked to the flow, so that each image showed different, random phases of the shedding. Because of the size of the image window, it was not possible to view two vortices simultaneously that had been shed from the wing, and so a Strouhal number could not be determined with these PIV realizations.

Table 1 shows several quantitative scalars determined from the PIV flow measurements. The maximum values of the Reynolds normal stresses correspond well with the LDA measurements of Jeffrey et al.⁵ In addition to these values, Table 1 shows an approximate downwash value, α_{app} . This value is determined by finding the angle of the average velocity vector at $x/c = 1.060$, a location generally downstream of the recirculating bubble. This value was not assumed to be the actual downwash angle because the imaged region only

**Fig. 3** Single actuated MiTE wake structure, mean velocity flowfield: a) $y/b = 0$, b) $y/b = 0.037$, and c) $y/b = 0.073$.

covered a portion of the wake. The scalar was simply meant to be a quantitative value for comparative purposes. The uncertainty in α_{app} is $\pm 0.9\%$. Clearly, the flow is significantly turned in the fully down position.

The spanwise variation was examined by applying single MiTEs downward at different locations relative to the sheet location. All other devices were fixed at the neutral position. Figure 3a shows the mean velocity field when the sheet was located at the center of the

midspan MiTE ($y/b = 0$). The flow structure was very similar to that of the full-span down position, with downturned flow, a larger separated region, and a more prominent suction-side vortex. The two vortices were larger than for the full-span down case, and they were located at approximately the same downstream position rather than staggered. Also, whereas the off-surface stagnation point was closer to the trailing edge in this partial-span condition, it also was shifted further toward the pressure surface. This suggests increased downwash, as indicated by the larger α_{app} in Table 1.

Figure 3b shows the wake flow to the side of the actuated flap at $y/b = 0.037$, one-half-device span past the tip of the flap. At first glance, this flow structure is nearly identical to that of the neutral condition, but there are subtle differences. The pressure-side vortex is slightly larger and stronger than in the neutral case, and the off-surface stagnation point is more toward the suction surface. This suggests that there is a small amount of upwash at this location, which is verified by the approximate downwash in Table 1. Both the qualitative comparison and the quantitative measurements show that the wake at this spanwise location was almost exactly the same as in the neutral case, implying that the spanwise influence of a single MiTE is small. This conclusion is further supported by the flow at $y/b = 0.073$ (Fig. 3c), which is virtually indistinguishable from the neutral case except for a tiny upwash in α_{app} .

The changes in α_{app} with spanwise position are evidence of the tip vortices produced at each end of the applied MiTE. These vortices produce a downwash behind the actuated surface and an upwash away from the edges. Away from the core of the vortex, the upwash decreases as $1/y$, which suggests that the spanwise influence away from an actuator would decay rapidly as y increases. This confirms why the significant MiTE influence is contained in a region approximately two flap spans wide.

The tip vortices explain why earlier pressure profile measurements showed a lift increment for spanwise positions near an actuated MiTE. The reason for the increment at the center of the device is obvious: The trailing edge of the flap is shifted toward the pressure surface. This increases the lift because of the Kutta condition, greater local wing camber, and greater local angle of attack. Downwash from the MiTE tip vortices reduces this lift somewhat, but the overall effect is positive. Away from the flap, there is no change in the airfoil contour, but the tip vortices produce an upwash at these locations. This increases the angle of attack slightly in this region, leading to a lift increment.

These conclusions were verified by conducting wake survey measurements with a pitot-static probe located 0.39 chords beyond the trailing edge. The surveys indicated that the major effects were localized to within two spans of the applied device.

The results presented here considered only static flaps and a rigid, nonoscillating wing. A separate set of experiments¹⁰ examined the effects of moving flaps. Those transient measurements, acquired only at $y/b = 0$, showed that a strong spanwise vortex was produced

behind the flap when the nondimensional MiTE actuation time was sufficiently short. This produced a momentary overshoot in the wake downwash angle. The stronger vortex likely also produced slightly greater spanwise effects. However, those results did not indicate any major difference in the qualitative flow structure for the stationary and actuated MiTE cases, and so additional spanwise variation is probably small. No experiments were conducted with an oscillating wing, but there is no reason to believe that the spanwise effects would be changed dramatically in that situation.

IV. Conclusions

The PIV measurements show that the spanwise MiTE influence is only significant within two flap spans. Thus, this device produces a localized effect of known value regardless of MiTE configuration, implying that these flaps could be modeled very simply.

Acknowledgments

This work was sponsored by the Air Force Office of Scientific Research. The collaborations of Ilan Kroo, Fritz Prinz, Byong-ho Park, Hak-tae Lee, and Stefan Bieniawski were critical to the research.

References

- ¹Lee, H., Kroo, I. M., and Bieniawski, S., "Flutter Suppression for High Aspect Ratio Flexible Wings Using Microflaps," AIAA Paper 2002-1717, April 2002.
- ²Solovitz, S. A., and Eaton, J. K., "Experimental Aerodynamics of Mesoscale Trailing-Edge Actuators," *AIAA Journal*, Vol. 40, No. 12, 2002, pp. 2538–2540.
- ³Liebeck, R. H., "Design of Subsonic Airfoils for High Lift," *Journal of Aircraft*, Vol. 15, No. 9, 1978, pp. 547–561.
- ⁴Jang, C. S., Ross, J. C., and Cummings, R. M., "Computational Evaluation of an Airfoil with a Gurney Flap," AIAA Paper 92-2708, June 1992.
- ⁵Jeffrey, D., Zhang, X., and Hurst, D. W., "Aerodynamics of Gurney Flaps on a Single-Element High-Lift Wing," *Journal of Aircraft*, Vol. 37, No. 2, 2000, pp. 295–301.
- ⁶Zerihan, J., and Zhang, X., "Force Enhancement of Gurney Flaps on a Wing in Ground Effect," AIAA Paper 2000-2241, June 2000.
- ⁷Park, B., "Miniaturization of Functional Mechanisms with SDM Processing," Ph.D. Dissertation, Dept. of Mechanical Engineering, Stanford Univ., Stanford, CA, Feb. 2002.
- ⁸Han, D., "Study of Turbulent Nonpremixed Jet Flames Using Simultaneous Measurements of Velocity and CH Distributions," Ph.D. Dissertation, Dept. of Mechanical Engineering, Stanford Univ., Stanford, CA, March 2001.
- ⁹Stanaway, S., McCroskey, W. J., and Kroo, I., "Navier–Stokes Analysis of Blunt Trailing Edge Airfoils," AIAA Paper 92-0024, Jan. 1992.
- ¹⁰Solovitz, S. A., and Eaton, J. K., "Experimental Aerodynamics of Mesoscale Trailing-Edge Actuators," Thermosciences Div., Dept. of Mechanical Engineering, Rept. TSD-149, Stanford Univ., Stanford, CA, Dec. 2002.

C. Pierre
Associate Editor